J Mater Sci (2007) 42:686–691
DOI 10.1007/s10853-006-0273-7

Magnetic properties of Re-substituted Ni–Mn ferrite nanocrystallites

Lijun Zhao · Hua Yang · Lianxiang Yu · Yuming Cui · Xueping Zhao · Shouhua Feng

Received: 7 May 2005 / Accepted: 14 October 2005 / Published online: 28 October 2006

Abstract The effect of Fe^{3+} ions substitutions by rare-earth ions on magnetic properties of nanocrystalline Ni–Mn ferrite prepared by emulsion method was investigated. X-ray diffraction pattern indicated the presence of cubic structure of spinel ferrite. The crystallite sizes increased with an increase in the heat treatment temperatures, while it decreased for the substitution of rare-earth ions. The magnetic properties were changed with types of rare-earth ions and heat treatment temperatures. Room temperature Mössbauer spectra can differentiate between superparamagnetism and ferrimagnetism in nature.

Introduction

The magnetic behavior of fine particles is of considerable interest both from a scientific and practical point of view [1, 2]. When the rare-earth ions substitute for Fe^{3+} ions in spinel ferrite, they may enter into the lattice and disturb grain, that is to say, rare-earth ions may make the grains fine [3]. Hence, rare-earth ions are doped into spinel ferrites to break the grain. It is known that the magnetic behavior of the ferromagnetic oxides is governed by the Fe^{3+}–Fe^{3+} interaction the spin coupling of the 3d electrons. By introducing RE^{3+} ions into spinel lattice, the RE^{3+}–Fe^{3+} interactions also appear 3d–4f coupling, which can lead to small changes in the magnetization and Curie temperature. The RE^{3+}–RE^{3+} interactions are very weak since they result from the indirect 4f–5d–5d–4f mechanism. In this paper, the influence of different types of rare-earth ions on the magnetic properties of Ni–Mn ferrite was investigated.

L. Zhao · H. Yang (✉) · L. Yu · Y. Cui
College of Chemistry, Jilin University, Changchun 130023, P.R. China
e-mail: huayang86@sina.com

X. Zhao
College of Physics, Jilin University, Changchun 130023, P.R. China

S. Feng
State Key Laboratory of Inorganic Synthesis and Prepartive Chemistry, Jilin University, Changchun 130023, P.R. China

Experimental procedure

Nanocrystalline samples of the nominal formula $Ni_{0.7}Mn_{0.3}RE_xFe_{2-x}O_4$ where $x = 0.0$ (US), 0.1 and RE^{3+} = La, Nd and Gd were prepared by the emulsion method, using analytically pure grade $Ni(NO_3)_2 \cdot 6H_2O$, $Fe(NO_3)_3 \cdot 9H_2O$, $Mn(NO_3)_2$ and RE_2O_3 as starting materials. PEG (molecular weight 20,000) was used as the surfactant. The nitrates were mixed with PEG to form the solution, then NH_4OH was dropped into the solution until Ph = 9.5 to form the precipitate. The precipitate was washed with distilled water for three times and dried at 90 °C for 7 h to prepare precursors. The precursors were calcined at different temperatures at atmosphere for 2 h, respectively. Nanocrystalline $Ni_{0.7}Mn_{0.3}RE_xFe_{2-x}O_4$ ferrites powders with different crystallite sizes were synthesized.

The structure and crystallite sizes are tested by X-ray diffractometer (XRD) in the 2θ range 25–65° using CuKα radiation (λ = 0.15405 nm). The type of X-ray diffractometer is SHIMADZU Co.Tokyo Japan. The database of the Joint Committee on Powder Diffraction Data was used for the interpretation of XRD spectra. The crystalline sizes

are calculated using Scherrer's relationship $D = k\lambda/B\cos\theta$, where ''D'' is the average diameter in nm, ''k'' is the shape factor, B are the half intensity width of the relevant diffraction peak and instrumental broadening, respectively. ''λ'' is the X-ray wavelength and θ is the Bragg's diffraction angle. The broadening of the (311) diffraction line of the ferrite materials was considered after computer fit of the X-ray data using the Gaussian line shape. The broadening of the diffraction line due to reduction of crystallite dimensions, i.e. B, was estimated by the relation, $B^2 = B_m^2 - B_s^2$, where B_m is the measured width of the diffraction line at its half maximum and B_s is the measured breadth of the line for the standard at its maximum. Mössbauer spectrum was recorded at 295 K by using a computerized Oxford MS-500 Mössbauer spectrometer of the electromechanical type in constant acceleration mode. A ^{57}Co source in a palladium matrix was used in a continuously distributed hyperfine magnetic field. A 25 μm thick high purity alpha iron foil was used for calibration. The experimental data were analyzed with a standard least square fitting program assuming Lorentzian line shapes. Magnetic measurements were carried out at room temperature using a vibrating sample magnetometer (VSM) (Digital Measurement System JDM-13) with a maximum magnetic field of 10,000 Oe.

Results and discussion

When the ferrite doped with a relatively small amount of rare-earth ions is synthesized at a higher temperature, besides the spinel phase, a foreign phase in a very small amount will be formed. Some was identified as the orthoferrite ($REFeO_3$) [4]. In our experiment, the samples were synthesized at relatively lower temperatures, so the extra phase was abstained. XRD patterns of $Ni_{0.7}Mn_{0.3}RE_xFe_{2-x}O_4$ ferrite nanocrystals synthesized at 600 and 850 °C are shown in Fig. 1. The peaks in the spectra indicate that nanocrystalline $Ni_{0.7}Mn_{0.3}RE_xFe_{2-x}O_4$ ferrites with no extra reflections are cubic structure of spinel ferrite. However, the diffraction peaks in $Ni_{0.7}Mn_{0.3}RE_{0.1}Fe_{1.9}O_4$ ferrites appear to be broaden as a result of incorporation of the rare-earth ions. Such results have been reported in the literatures about the spinel ferrites doped with rare-earth ions [5, 6]. Further, the increase in intensity of X-ray diffraction shows improved crystallinity of nanocrystals. This indicates gradual increase in the crystalline sizes as a function of heat treatment temperatures.

The crystallite sizes of $Ni_{0.7}Mn_{0.3}RE_xFe_{2-x}O_4$ ferrite nanocrystals varied with heat treatment temperatures and types of rare-earth ions are listed in Table 1. It can be easily got that the crystallite sizes are increased with the heat treatment temperatures for all the samples. The crystal structure will be more complete with the adsorption of energy, so the crystallite sizes increase with the heating treatment temperatures for all the samples. The crystallite sizes decreased when RE^{3+} ions were doped into Ni–Mn ferrites. Figure 2 shows the dependence of crystallite sizes of Ni–Mn ferrite on the rare-earth types and heat treatment temperatures. From Fig. 2, the variational law of crystallite sizes with heat treatment temperatures and types of rare-earth ions can be observed obviously. First, it is well known the shrinkage of lanthanide. The radii of Re^{3+} = La, Nd and Gd are 1.06, 0.995 and 0.938 Å, respectively. And the radii of RE^{3+} ions are larger than that of Fe^{3+} ions 0.64 Å. When some Fe^{3+} ions at ferrite lattice site are substituted by some RE^{3+} ions, the lattice parameters will be changed [3, 7–9]. The variation of lattice parameters will lead to the lattice strains, which produce the internal stress [5, 9, 10]. Such a stress hinders the growth of grains, so that the grain sizes of the samples doped with rare-earth ions are smaller than that of Ni–Mn ferrite nanocrystal. Secondly, the RE^{3+} ions have empty or half-filled or fully filled 4f electron shell with stable structure, so the sample with rare-earth ions has high thermal stability. The larger bond intensity of RE^{3+}–O^{2-} as compared with that of Fe^{3+}–O^{2-}. The bond intensity of Fe^{3+}–O^{2-}, La^{3+}–O, Nd^{3+}–O and Gd^{3+}–O are 390.4 ± 17.2 (kJ mol^{-1}), 799 ± 4 (kcal mol^{-1}), 703 ± 13 (kcal mol^{-1}) and 719 ± 10 (kJ mol^{-1}), respectively. More energy is needed to make R ions enter into lattice and form the bond of RE^{3+}–O^{2-}. Bond energy is a part of inner energy. During the process of bond break or

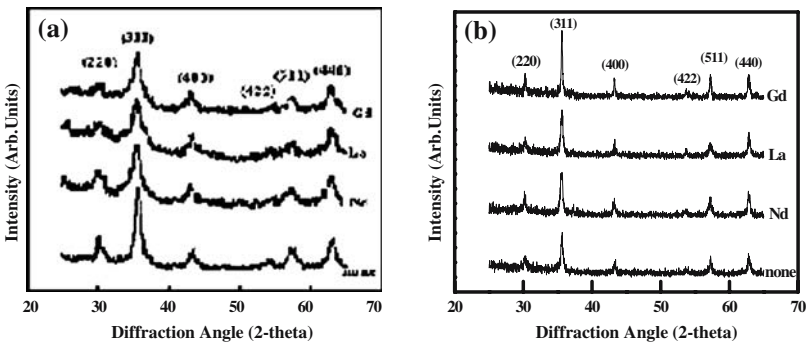

Fig. 1 XRD patterns of $Ni_{0.7}Mn_{0.3}RE_xFe_{2-x}O_4$ ferrite nanocrystals synthesized at: (**a**) 600 °C, (**b**) 850 °C

Table 1 Crystallite sizes of $Ni_{0.7}Mn_{0.3}RE_xFe_{2-x}O_4$ ferrite nanocrystals varied with heat treatment temperatures and types of rare-earth ions

RE^{3+}	Crystallite sizes (nm)		
	600 °C	800 °C	850 °C
None	13.8	34.4	47.5
La	10.1	11.4	32.5
Nd	10.7	15.0	39.6
Gd	7.8	21.0	38.6

formation, inner energy will be changed in the chemical reaction. If the bulk work is small enough and can be neglected, the variation of enthalpy will be equal to the variation of inner energy, i.e. $\Delta H_{298.15} \approx \Delta U_{298.15}$. The variation of bond energy will directly lead to the variation of enthalpy. So the increase of bond energy will induce the increase of inner energy, i.e. more energy is needed to form the bond of RE^{3+}–O^2. The higher thermal stability of the RE^{3+}-doped samples relatives to Ni–Mn ferrite, and hence more energy is needed for the RE^{3+}-doped samples to complete crystallization and grains grow. Finally, the doped RE^{3+} ions, during the sintering process, will diffuse to the grain boundaries and form an isolating ultra-thin layer around the grains. The primary effect of segregation process on grain boundary is to suppress the grain growth by limiting grain mobility, and the smaller crystallite sizes are obtained.

In our explanations, there is an assumption that some RE^{3+} ions are substituted for Fe^{3+} ions and resided at grain boundary. The above mentioned assumption may be testified by the data listed in Table 2. The Lattice parameters of $Ni_{0.7}Mn_{0.3}RE_xFe_{2-x}O_4$ ferrite nanocrystals calcined at 850 °C are given in Table 2. It is clearly that the lattice parameters decreased for all substituted samples relative to un-substituted sample. If the lattice parameters are

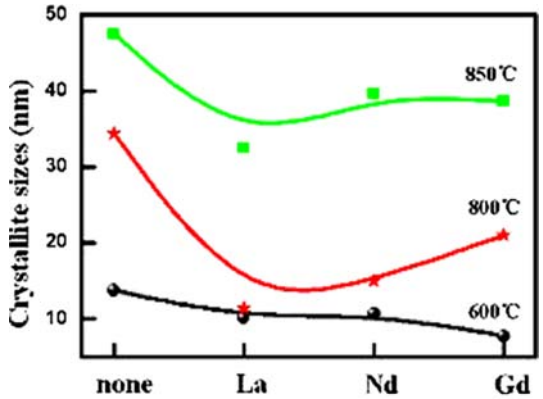

Fig. 2 Dependence of crystallite size on types of rare-earth ions and heat treatment temperatures

increased, it may be the incorporation of rare-earth ions in spinel lattice. However, the experimental result is that the lattice parameters are decreased with the incorporation of rare-earth ions. The removal of the rare-earth ions from the spinel lattice may explain why the lattice parameters are decreased. During the sintering process, some RE^{3+} ions will diffuse to the grain boundaries and form an isolating ultra-thin layer around the grains. From the values of lattice constant, we can estimate the residing amount on grain boundary. The lattice constants decreased with an increase in the radii of substituted rare-earth ions. If the incorporation amount of rare-earth ions in spinel lattice is little, residing amount of rare-earth ions on grain boundary will be much, and then the lattice parameter is small. The Gd^{3+}-doped sample has the largest lattice constant relative to that of La^{3+}- and Nd^{3+}-doped samples, so the order of residing amount is La, Nd and Gd.

Figure 3 shows the hysteretic curves for $Ni_{0.7}Mn_{0.3}RE_xFe_{2-x}O_4$ ferrite nanocrystals synthesized at 600 and 800 °C. The magnetic parameters obtained by hysteretic curves are listed in Table 3. For the samples calcined at 600 °C, the values of Hc and Mr are zero because of the presence of superparamagnetism. In addition, the Hc and Mr values of the Ni–Mn ferrite calcined at 800 °C are larger than that of Ni–Mn ferrite calcined at 850 °C. For RE^{3+}-doped samples calcined at 800 °C, the values of Hc and Mr are less than that of Ni–Mn ferrite. The Hc and Mr values of the RE^{3+}-doped samples increase with calcination temperatures. For the RE^{3+}-doped samples calcined at 850 °C, the values of Hc and Mr are larger than that of Ni–Mn ferrite. The variational law also can be observed from Fig. 4a. Probably the critical diameter of these samples is near 35–40 nm, which explains the increasing and decreasing of coercivity values [11, 12]. When the particle size is much larger than the critical size of a single-domain, the coercivity is decided by magnetic displacement, so the value of coercivty is small. When the particle size is reduced to the critical size of single-domain, the coercivity is decided by magnetic domain rotation, so the coercivity reaches the maximum. When the particle size is less than the critical size of single-domain, the coercivity will be decreased for the existence of superparamagnetism. Moreover, rare-earth ions can't all enter into the ferrite lattice, as the lager radii of RE^{3+} ions relative to Fe^{3+} ions. So some RE^{3+} ions may reside at grain boundary and form isolating ultra-thin layer around the grains during the sintering process. The presence of isolating ultra-thin layer at grain boundary inhibits the motion

Table 2 The lattice parameters a of $Ni_{0.7}Mn_{0.3}La_xFe_{2-x}O_4$ ferrite nanocrystals calcined at 850 °C

RE^{3+}	None	La	Nd	Gd
a (Å)	8.3796	8.3648	8.3660	8.3681

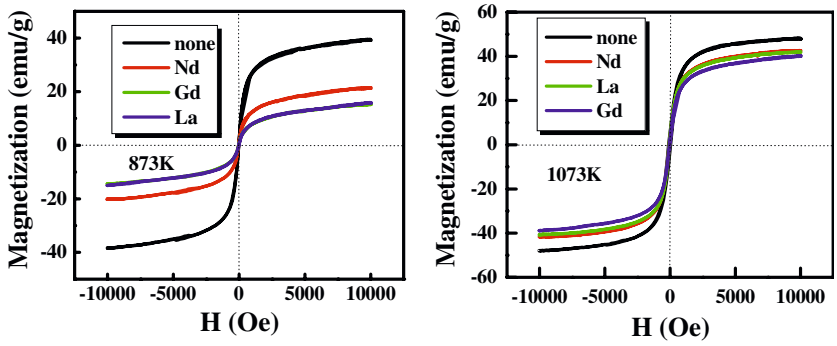

Fig. 3 The hysteretic curves for $Ni_{0.7}Mn_{0.3}RE_xFe_{2-x}O_4$ ferrite nanocrystals synthesized at 600 and 800 °C

Table 3 Effects of RE^{3+} ions and crystallite sizes on the magnetic properties

RE^{3+}	*D* (nm)	Ms (emu/g)	Hc (Oe)	Mr (emu/g)
None	13.8	39.5	0	0
	34.4	48.3	76.9	3.2
	47.5	55.6	47.6	2.8
La	10.1	15.3	0	0
	11.4	42.0	41.2	2.4
	32.5	44.3	60.4	3.6
Nd	10.7	21.4	0	0
	15.0	42.7	22	1.9
	39.6	49.3	53	3.8
Gd	7.8	16.0	0	0
	21.0	40.2	30	1.2
	38.6	48.2	54.6	3.1

of domain walls. The isolating ultra-thin layer will be more stable with the increasing heat treatment temperatures, so the Hc values of RE^{3+}-doped samples increase with the heat treatment temperatures.

It can be seen from Table 3 that the Ms values of all samples increase with an increase in crystallite sizes. At the same calcination temperature, the Ms values of the samples doped with RE^{3+} ions are less than that of un-doped one. This may be due to smaller crystallite sizes for RE^{3+}-doped samples. And some RE^{3+} ions may reside at grain boundary, so the Fe^{3+}–Fe^{3+} interactions are decreased for reduction in the concentration of Fe^{3+} ions on lattice sites. Before the experiment, we expect that the Ms values will change with the magnetic moment of RE^{3+} ions. In fact, the RE^{3+}-doped samples with similar crystallite sizes have similar Ms values. The results may be deduced that the RE^{3+}-doped contents are 10% of Fe^{3+} contents. The substitutional amount can't too large, or the ferrite will not keep the cubic structure of spinel ferrite. The micro-substitution is not enough to change the saturation magnetization significantly. From Table 3 and Figs. 3 and 4, we can observe that the Nd^{3+}-doped sample has the highest Ms value relative to the other substituted samples. As assumed above, RE^{3+} ions can't all enter into ferrite lattice, but some reside at the grain boundaries. This may increase the magnitude of magnetic interactions and cause the increase of saturation magnetization. So the Ms value of Nd^{3+}-doped sample is larger than that of Gd^{3+}-doped one. The Ms for Nd^{3+}-doped sample is larger than that of La^{3+}-doped one, which may be due to infinite effects.

Figure 5 shows the Mössbauer spectra of the RE^{3+}-doped samples for calcined at 800 and 600 °C. As evident from the Fig. 5I, the spectra consist of Zeeman sextets, however there are some superparamagnetic phase in pattern a. Fig. 5II shows that the spectra consist of quadrupole doublets, but there are some ferromagnetic phase in the pattern c.

Table 4 shows the room temperature Mössbauer spectra parameters for RE^{3+}-doped samples. δ, ΔE, B and A_0 represent isomer shift, quadrupole shift, hyperfine field and

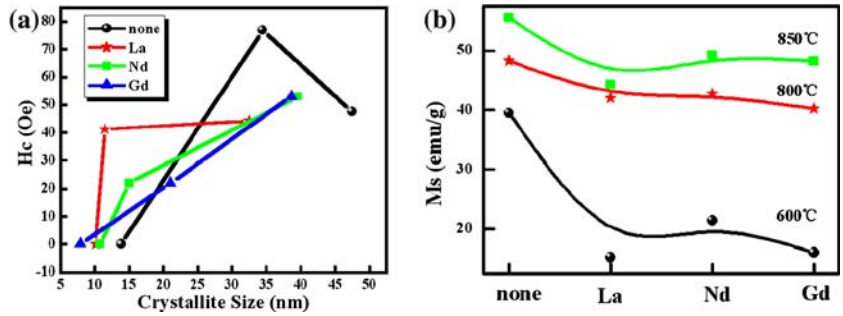

Fig. 4 (**a**) The values of coercivity varied with crystallite sizes (**b**) The values of Ms varied with type of rare-earth ions at different heat treatment temperatures

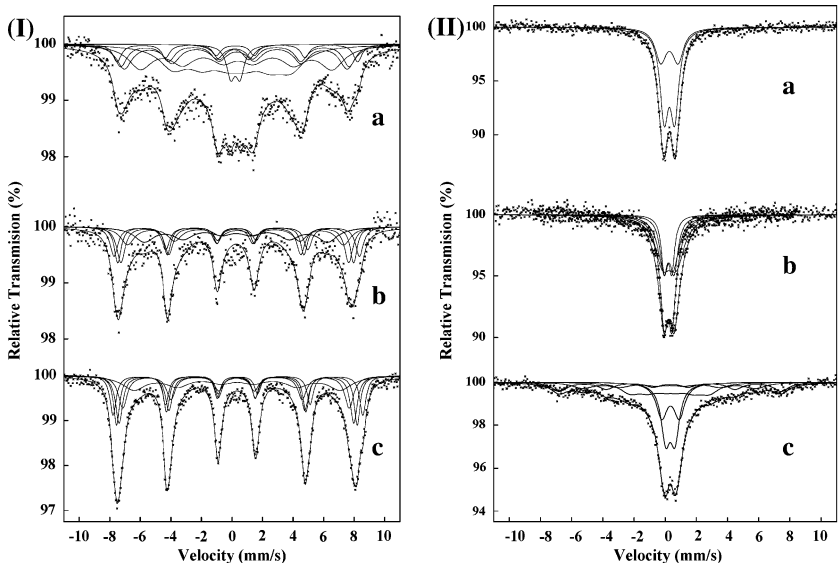

Fig. 5 The Mössbauer spectra of the samples calcined at 800 °C (**I**) and 600 °C (**II**): a, RE3+ = La; b, R = Nd; c, R = Gd

fractional area of the pattern, respectively. Table 4 illustrates that the δ values of A-sites are less than that of B-sites. This conclusion has been proved by many literatures [13–15]. The values of ΔE indicate the degree of deviating from cubic symmetrical structure. The absolute values of ΔE will be increased with the decreasing particle sizes, and the asymmetrical electric fields surrounding the Mössbauer nucleus will be strengthened along with the decreasing particle sizes. Because the particle sizes are small, the crystallization will be incomplete. The value of B (II) is larger than that of B (I). This may result from that the magnetic properties are increased with the crystallite sizes. This can be proved by the result of VSM. In addition, the presence of superparamagnetic phase C_A and C_B in samples also makes the decrease of the hyperfine field. From the B values in Table 4, it can be observed that the B value is proportional to the effective magnetic moment of rare-earth ions. The sample with Gd^{3+} ions has the maximum B value, however the sample with La ions has the minimum value of hyperfine field. This can be explained as follows: the hyperfine magnetic field can be written as $B = au_{Fe} + b\bar{u}$, where a and b are proportionality constants, u_{Fe} is the magnetic moment of the Fe atom and $\bar{u}$ is the average magnetic moment of compound [16]. So the increase in B could be attributed to the increase in the average magnetic moment $\bar{u}$ of the compound. The effective moment of rare-earth ion for RE^{3+} = La, Nd and Gd are 0, 3.64 and 7.94 μ_B, respectively, so the sample with Gd^{3+} ions has the maximum B value. The difference in B for the two magnetic sites is due to the difference in crystal structure, since the atomic contribution is the same for both sites.

From the percent of the absorption area of the Mössbauer spectra, we can decide the cation distribution. The fraction of Fe^{3+} ions at the tetrahedral A and octahedral B sites were determined using the area of Mössbauer spectra. For stoichiometric ferrite it is easy to estimate the cation distribution, but it becomes rather difficult for mixed ferrites, since they contain mixtures of more than one cation other than iron.

Conclusions

X-ray diffraction patterns indicated the presence of single cubic spinel phase in nanocrystalline $Ni_{0.7}Mn_{03}RE_{0.1}Fe_{1.9}O_4$ ferrites. The crystallite sizes and saturation magnetization increased with heat treatment temperatures and decrease for

Table 4 The room temperature Mössbauer spectra parameters for RE^{3+}-doped samples

Sample	Sublattice	δ (mm s^{-1})	ΔE (mm s^{-1})	B (kOe)	A_0 (%)
La (I)	A	0.21	0.14	351.0	0.41
	B	0.35	0.1	443.1	0.49
	C_A	0.18	1.88	—	0.05
	C_B	0.27	0.62	—	0.04
La (II)	C_A	0.31	0.67	—	0.66
	C_B	0.32	1.10	—	0.34
Nd (I)	A	0.26	0.006	470.5	0.41
	B	0.33	0.05	436.1	0.59
Nd (II)	C_A	0.29	0.65	—	0.37
	C_B	0.33	0.89	—	0.63
Gd (I)	A	0.34	0.04	473.9	0.39
	B	0.39	0.01	467.2	0.61
Gd (II)	A	0.32	0.04	343.9	0.15
	B	0.38	0.05	299.2	0.39
	C_A	0.37	0.59	—	0.26
	C_B	0.39	1.12	—	0.20
Error		±0.02	±0.02	±1.0	±0.02

the substitution of rare-earth ions. Moreover, the Ms values are independent of the effective magnetic moment of rare-earth ions. The order of residing amount can be estimated by lattice parameters. The variational laws of Hc and Mr prove further that rare-earth ions can't enter into ferrite lattice totally, but some reside at the grain boundaries. Room temperature Mössbauer spectra shows that B value is proportional to the effective magnetic moment of rare-earth ions.

Acknowledgements This work is supported by National Natural Science Foundation of China (NNSFC) (Grant No. 50372025, 50572033).

References

1. Richter HJ (1999) J Phys D: Appl Phys 32:R 147
2. Gleiter H, Weissmuller J, Wollersheim O, Wurschum R (2001) Acta Mater 49:737
3. Satar AA, Samy AM, El-Ezza RS, Eatah AE (2002) Phys Stat Sol (a) 193(1):86
4. Rezlescu N, Rezlescu E, Pasnicu C, Craus ML (1994) J Phys: Condens Matter 6:5707
5. Yang H, Zhao L, Yang X, Shen L, Yu L, Sun W, Yan Y, Wang W, Feng S (2004) J Magn Magn Mater 271:230
6. Cheng F, Jia J, Xu Z, Zhou B, Liao C, Chen L, Zhao H (1999) J Appl Phys 86:2727
7. Rezlescu N, Rezlescu E, Pasnicu C, Craus ML (1994) J Magn Magn Mater 136:319
8. Rezlescu N, Rezlescu E, Popa PD, Rezlescu L (1998) J Alloy comp 275–277:657
9. Sattar AA, Wafik AH, El-Shokrofy KM, El-Tabby MM (1999) Phys Stat Sol (a) 171:563
10. Yang H, Wang Z, Song L, Zhao M, Wang J, Luo H (1996) J Phys D: Appl Phys 29:2574
11. Albuquerque AS et al (2000) J Appl Phys 87(9):4352
12. Cullity BD (1972) Introduction to magnetic material. Addision-Wesley, London
13. Tang H, Du YW, Qiu ZQ, Walker JC (1998) J Appl Phys 63:4105
14. Chae KP, Kim WK, Lee SH, Lee YB (2001) J Magn Magn Mater 232:133
15. Li X, Kutal C (2003) J Allo Comp 349:264
16. Vincze I, Campell IA, Meyer AJ (1974) Solid State Commun 15:1495